# Analyst

Accepted Manuscript

This article can be cited before page numbers have been issued, to do this please use: Z. Dai, H. Gao, S. Liu, Z. Wang and L. Shi, *Analyst*, 2018, DOI: 10.1039/C8AN00667A.

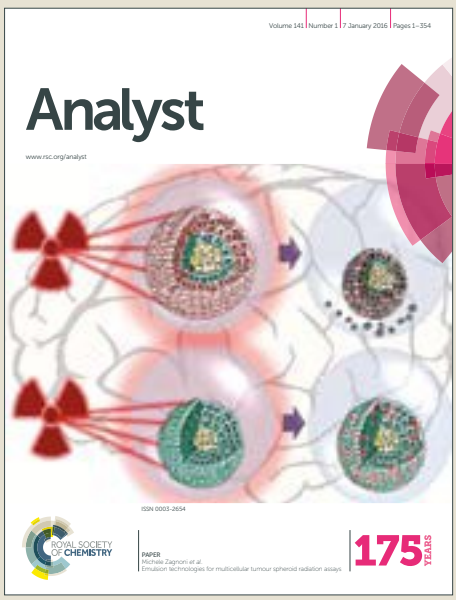




ROYAL SOCIETY OF CHEMISTRY

rsc.li/analyst

View Article Online
DOI: 10.1039/C8AN00667A

Journal Name

COMMUNICATION

# A novel electrochemiluminescence biosensor based on S-doped yttrium oxide ultrathin nanosheets for detection of anti-Dig antibodies

Received 00th January 20xx,
Accepted 00th January 20xx

DOI: 10.1039/x0xx00000x

www.rsc.org/

Huan Gao[a], Suli Liu[b], Zhaoyin Wang[a], Ling Si*[a], and Zhihui Dai*[a,c]

**New S-doped yttrium oxide ultrathin nanosheets (NSs) were synthesized which had good electrochemiluminescence (ECL) properies. Through combining this NSs with small molecule linked DNA as the substrate, a novel ECL biosensor was constructed for detection of protein biomarkers with an acceptable performance.**

Nanocrystal-based electrochemiluminescence (ECL) has attracted an increasing attention in bioanalysis due to the strong size-dependent electronic, optical, and electrochemical properties of the luminescent nanocrystals (NCs).[1-3] Among them, the semiconductor nanocrystals, such as CdS, CdSe, and PbS were extensively chosen as ECL emitters due to their narrow emission band, good photostability, and high quantum yields.[4-6] However, heavy-metal elements (e.g., Cd and Pb) are highly cytotoxic which lead to some restrictions of these NCs in their applications.[7,8] Thus, the development of environmentally friendly and low-toxicity or even nontoxic ECL emitters for bioassays has been an urgent need. Traditionally, ECL is a light emitting process which generates excited states by energetic electron transfer occurring in the vicinity of the working electrode.[9] Therefore, yttrium oxide ($Y_2O_3$) NCs are typically considered as an ideal ECL substrate because they can harvest electron to generate electron-hole pairs, leading to the boost of charge-transfer and the enhancement of ECL response.[10,11] Especially, the introduction of sulphur (S) atoms into $Y_2O_3$ nanosheets (NSs) can also affect the electron-hole recombination statistics, which may result in new properties. In our work, we introduce S atoms into $Y_2O_3$ ultrathin NSs, providing a viable approach to gain a novel ECL emitter at the atomic level.

In recent years, the development of rapid, low cost and point-of-care approaches for the quantitative detection of antibodies has become more prevalent due to its dramatically impact on global health.[12,13] A variety of methods, such as electrochemistry, fluorescence, have been developed for the quantitative detection.[14-16] However, these methods are limited due to their low detection limits or time-consuming procedures.[17] Among various alternatives, ECL analysis based on single or several-atom-thick NSs has raised concerns due to its low background, simple instrument, and high sensitivity of analysis method, as well as the bigger specific surface area, more active sites and good ECL properties of materials.[18-20] Herein, a novel ECL biosensor based on S-doped $Y_2O_3$ ultrathin NSs was constructed for quantitative detection of anti-Dig antibodies. This proposed ECL biosensor used small molecule linked DNA as the flexible recognition elements to recognize anti-Dig antibodies (Scheme 1). This method produced prominent steric hindrance to impede the electron transfer of ECL reagents towards the electrode surface. Based on the variation of ECL intensities before (a in Scheme 1) and after (b in Scheme 1) anchoring the antibodies, a sensitive and simple biosensor was designed, which exhibited a good performance. The results of this study suggested that new two-dimensional luminescent rare earth materials may possess enhanced ECL performances, and can be applied in related ECL bioassays.

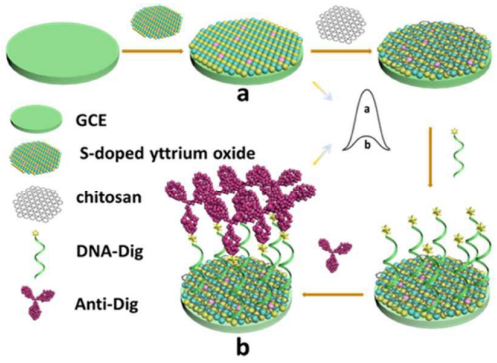


**Scheme 1** Schematic presentation of the proposed ECL biosensor for detecting anti-Dig antibodies.

*a Jiangsu Collaborative Innovation Centre of Biomedical Functional Materials and Jiangsu Key Laboratory of Biofunctional Materials, school of Chemistry and Materials Science, Nanjing Normal University, Nanjing, 210023, P. R. China. E-mail: daizhihuii@njnu.edu.cn and 07162@njnu.edu.cn. Tel./Fax: +86-25-85891051.*
*b Department of Chemistry, Nanjing Xiaozhuang College, Nanjing 211171, P. R. China.*
*c. Nanjing Normal University Centre for Analysis and Testing, Nanjing, 210023, P. R. China*
†Electronic Supplementary Information (ESI) available: Experimental section and supplementary results. See DOI: 10.1039/x0xx00000x

View Article Online
DOI: 10.1039/C8AN00667A



X-ray energy dispersive spectroscopy (EDS) analysis (Fig. S1, ESI) shows that the sample is composed of yttrium (Y), oxygen (O) and S elements. The X-ray diffraction (XRD) pattern of the sample displays the major diffraction peaks corresponding to the $Y_2O_3$ (JCPDS 65-3178) (Fig. S2, ESI). Meanwhile, some slight differences are also observed. This may be due to the low concentration of S uniformly substitution into the $O^{2-}$ sites or interstitial sites in $Y_2O_3$ lattice.[21] The structure of S-doped $Y_2O_3$ NSs is further confirmed by the transmission electron microscopy (TEM) analysis and elemental mapping. The near transparency image of the NSs in Fig. 1A is an indication of the formation of the ultrathin structure. The elemental mapping in Fig. 1B shows the uniform distribution of Y, O, and S across the NSs area. The thickness

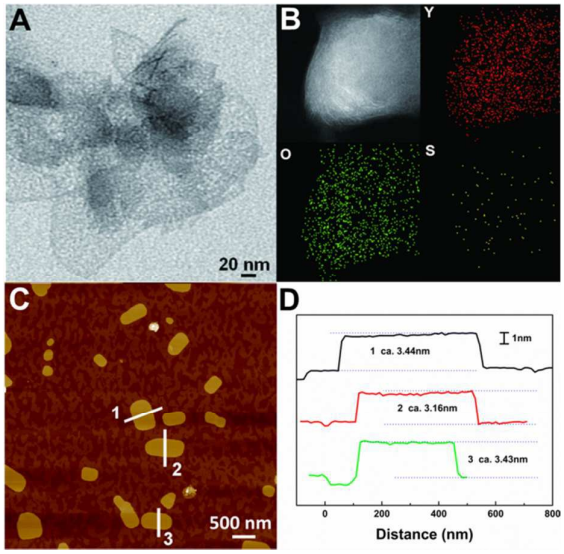


**Figure. 1** (A) TEM image of the S-doped $Y_2O_3$ NSs, (B) Elemental mapping of a selected area of the S-doped $Y_2O_3$ NSs, (C) AFM image and (D) height profiles of the S-doped $Y_2O_3$ NSs. The profiles 1, 2, and 3 in Fig. 1C correspond to the lines labelled as black, red and green lines in Fig. 1D.

of the S-doped $Y_2O_3$ NSs (Fig. 1C and D) is approximately 3.34 nm, which is measured by atomic force microscopy (AFM).[22]

The ECL potential spectra with different modifications were obtained in 0.1 M PBS buffer, between -1.36 and -2.0 V, at a scan rate of 100 mV $s^{-1}$ with 50 mM $K_2S_2O_8$ as a co-reactant. Fig. 2A shows the ECL behaviours under above experimental conditions for bare glassy carbon electrode (GCE, black line), S-doped $Y_2O_3$ nanowires (NWs, red line), $Y_2O_3$ NSs (green line) and S-doped $Y_2O_3$ NSs (blue line). The initial potential of S-doped $Y_2O_3$ NSs is -1.45 V. The tests above indicate that the relative ECL intensities of the studied materials increase in the following order: bare GCE < S-doped $Y_2O_3$ NWs < $Y_2O_3$ NSs < S-doped $Y_2O_3$ NSs modified GCEs. Obviously, the ECL intensity of the S-doped $Y_2O_3$ NSs is greater than those of the other NCs, indicating that the S-doped $Y_2O_3$ NSs dramatically enhance the ECL activity.

In addition to the ECL intensity, durability is another important parameter to evaluate the ECL materials. Fig. 2B presents the continuous high ECL emission of the S-doped

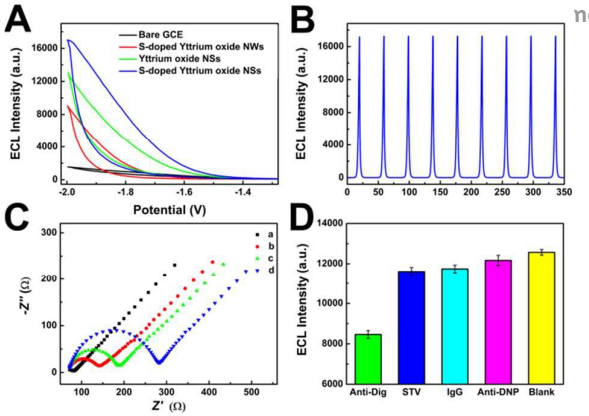


**Figure. 2** (A) ECL potential curve of Bare GCE (black line), S-doped $Y_2O_3$ NWs (red line), $Y_2O_3$ NSs (green line), S-doped $Y_2O_3$ NSs (blue line) modified GCEs in 0.1 M PBS buffer containing 50 mM $K_2S_2O_8$ and 0.1 M KCl. (B) Stability of ECL response from S-doped $Y_2O_3$ NSs modified GCE during eight cycles of continuous CV scans (n = 3) and (C) Nyquist diagrams of (a) bare GCE, (b) Cs-S-doped $Y_2O_3$ NSs/GCE, (c) Capture DNA/ Cs-S-doped $Y_2O_3$ NSs/GCE, (d) Anti-Dig/DNA/Cs-S-doped $Y_2O_3$ NSs/GCE. (D) ECL responses of the biosensor towards anti-Dig antibodies (10 nM), streptavidin (100 nM), human immunoglobulin G (100 nM), anti-dinitrophenol (100 nM) and blank for contrast.

$Y_2O_3$ NSs for nine cycles, demonstrating that the S-doped $Y_2O_3$ NSs has long-term ECL stability. Besides, the relative standard deviation (RSD) is calculated to be 0.7%. Moreover, the ECL intensity and stability of $Y_2O_3$ NSs and S-doped $Y_2O_3$ NWs are also presented in Fig. S3. By comparison, the S-doped $Y_2O_3$ NSs are more suitable for ECL application than $Y_2O_3$ NSs and S-doped $Y_2O_3$ NWs.

The characterizations of $Y_2O_3$ NSs and S-doped $Y_2O_3$ NWs have been shown in Fig. S4. According to the previous reports, the $Y_2O_3$ can be used as an acceptor or host material and harvest surrounding electrons to generate electron-hole pairs.[23-26] Then, the high energy electrons from electrode directly inject the conduction band (CB) of $Y_2O_3$ NSs, which results in the transfer of electrons from the CB to the valence band (VB); subsequently, co-reactant also takes part in the reaction and produces electron holes. The two responses react with each other and generate electron-hole pairs, leading to the boost of charge separation and the enhancement of ECL response.[27] Especially, when the S atoms are introduced into ultrathin $Y_2O_3$ NSs, some significant changes in electronic structure will occur. This might originate from that S atoms partly substitute for the original O atoms, which contributes more active sites and minor disorder, promoting the electron transmission.[28] The subtle distortion of the atomic arrangement can offer abundant unsaturated O atoms as active sites for ECL, which can improve the intrinsic conductivity and optimize ECL performance on the basis of guaranteed robust electron transfer.[29,30] Thus, it can be speculated that the $Y_2O_3$ ultrathin NSs harvest surrounding electrons and translate them into excited state, then, persulfate ($S_2O_8^{-}$) is reduced to hole donor ($SO_4^{\bullet-}$), and leading to the enhancement of ECL response. Furthermore, doping S into $Y_2O_3$ ultrathin NSs leads to the higher ECL intensity and stability.[31]

The effects of some parameters on ECL response are studied to identify the optimal conditions for the construction of biosensor (Fig. S5, ESI). When the concentration of capture DNA is 1 μM and incubation time of anti-Dig antibodies is 45 minutes, the ECL intensity is nearly steady. Electrochemical

View Article Online
DOI: 10.1039/C8AN00667A




impedance spectroscopy shows the stepwise assembly of the ECL sensor (Fig. 2C).[32] The diameters of the semicircle grow increasingly from curve a to curve d, which reflects the improvement of electron transfer resistance ($R_{et}$). The bare GCE shows the lowest $R_{et}$ value (Fig. 2C, curve a). When S-doped $Y_2O_3$ NSs coat on the surface of GCE, the $R_{et}$ value increases (Fig. 2C, curve b), which is attributed to the reason that the NSs block the electron transfer to the surface of the electrode. After the capture DNA links to S-doped $Y_2O_3$ NSs modified GCE by amino bond, a bigger semicircle forms and shows that DNA molecules can hinder the way of $[Fe(CN)_6]^{3-/4-}$ to the electrode (Fig. 2C, curve c). With the anti-Dig antibodies connect with

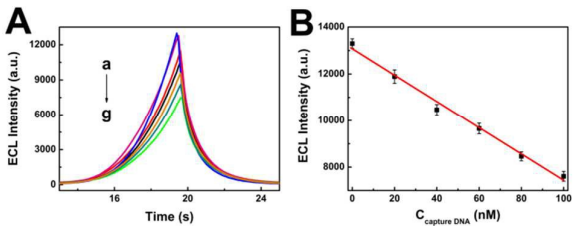


**Figure 3** (A) ECL intensity-time curves of the proposed ECL biosensor with different concentrations of anti-Dig antibodies (from top to bottom: 0, 1, 20, 40, 60, 80, 100 nM) in 0.1 M PBS buffer containing 50 mM $K_2S_2O_8$ and 0.1 M KCl. (B) Linear calibration curve between ECL intensity and the logarithm of the anti-Dig antibodies concentration.

Dig small molecules, the $R_{et}$ value increases remarkably (Fig. 2C, curve d).

The selectivity of this ECL biosensor is investigated by different analytes that includes human immunoglobulin G (IgG), streptavidin (STV) and rabbit polyclonal anti-dinitrophenol (anti-DNP) under the same experiment condition (Fig. 2D). These results suggest that this biosensor has a better performance for testing anti-Dig antibodies concentration and a good selectivity of ECL assay method. The ECL intensity is found to decrease severely with increasing concentrations of anti-Dig antibodies from 1 to 100 nM (Fig. 3A). Fig. 3B exhibits a good linear relationship with the same range of anti-Dig antibodies concentrations. The regression equation is $I = 13086.6 - 56.86c$ with a correlation coefficient of 0.995, where $c$ is the concentration of anti-Dig antibodies concentrations (nM). The detection limit is calculated to be 0.72 nM with the 3σ rule (σ is the standard deviation in the blank solution after repeated measurements) (LOD=3σ/k). The ECL biosensor presents a better analytical ability based on S-doped $Y_2O_3$ ultrathin NSs as signal donor. Several analytical approaches for detecting anti-Dig antibodies have been summarized in Table S1. It can be found that the linear range and detection limit of our proposed biosensor are better than or at least comparable to those of others. Recovery detections are carried out to demonstrate the feasibility of this biosensor in practical applications. Different concentrations of anti-Dig antibodies are spiked in health human serum, and then obtained with our method. The experimental results are listed in Table 1. There are no serious deviations, indicating that this ECL biosensor is suitable for detecting anti-Dig antibodies in real samples.

**Table 1** Serum samples tests of anti-Dig antibodies.

| Sample | Anti-Dig added (nM) | Anti-Dig found (nM) | Recovery (%) | RSD (%, n=3) |
|---|---|---|---|---|
| **Sample1** | 70 | 71.15 | 101.64 | 3.52 |
| **Sample2** | 30 | 28.94 | 96.46 | 2.03 |
| **Sample3** | 1 | 1.02 | 102.53 | 1.39 |

## Conclusions

In summary, we synthesized an ultrathin S-doped $Y_2O_3$ NSs and used its intrinsic ability of robust electron transfer as a good substrate for ECL application. The superb electron harvest, subtle distortion and flat superficial area offered more active sites and facilitated the rapid transport of electrons to the NSs. Hence, the S-doped $Y_2O_3$ NSs showed a good ECL performance. Therefore, based on steric hindrance inhibition of electron transfer, using Dig linked DNA to grapple anti-Dig antibodies, we combined S-doped $Y_2O_3$ ultrathin NSs with molecule-protein recognize interaction to construct this sensor, which provided low-cost and convenient ECL assay. This work presented a novel ultrathin S-doped $Y_2O_3$ NSs for ECL application that showed a good analytical performance. Considering that this method of detecting antibodies was used in ECL for first time, this biosensor may provide a powerful perspective for antibody detection.

## Conflicts of interest

There are no conflicts to declare.

## Acknowledgements

This work was supported by the NSFC (21625502, 21475062, 21205061). We appreciate the financial support from the PAPD of Jiangsu Higher Education Institutions.

## Notes and references

1 Y. Chen, S. W. Zhou, L. L. Li and J. J. Zhu, Nano Today, 2017, **12**, 98.
2 Z. Y. Liu, W. J. Qi and G. B. Xu, Chem. Soc. Rev., 2015, **44**, 3117.
3 K. D. Gilroy, A. Ruditskiy, H. C. Peng, D. Qin and Y. N. Xia, Chem. Rev., 2016, **116**, 10414.
4 J. Wang, X. Jiang and H. Han, Biosens. Bioelectron., 2016, **82**, 26.
5 D. Q. Liu, L. Wang, S. H. Ma, Z. H. Jiang, B. Yang, X. J. Han and S. Q. Liu, Nanoscale, 2015, **7**, 3627.
6 W. P. Li, L. Li, S. G. Ge, X. R. Song, L. Ge, M. Yan and J. H. Yu, Chem. Commun., 2013, **49**, 7687.
7 Q. F. Zhai, H. H. Xing, X. W. Zhang, J. Li and E. K. Wang, Anal. Chem., 2017, **89**, 7788.
8 M. X. Li, W. Zhao, G. S. Qian, Q. M. Feng, J. J. Xu and H. Y. Chen, Chem. Commun., 2016, **52**, 14230.
9 L. L. Li, Y. Chen and J. J. Zhu, Anal. Chem., 2017, **89**, 358.
10 Y. Luo, A. Habrioux, L. Calvillo, G. Granozzi and N. Alonso-Vante, ChemCatChem., 2015, **7**, 1573.
11 Q. L. Dai, M. E. Foley, C. J. Breshike, A. Lita and G. F. Strouse, J. Am. Chem. Soc., 2011, **133**, 15475.

View Article Online
DOI: 10.1039/C8AN00667A


12 Y. Peng, X. Li, R. Yuan and Y. Xiang, Chem. Commun., 2016, **52**, 12586.
13 S. S. Mahshid, S. Camiré, F. Ricci and A. Vallée-Bélisle, J. Am. Chem. Soc., 2015, **137**, 15596.
14 A. Vallée-Bélisle, F. Ricci, T. Uzawa, F. Xia and K. W. Plaxco, J. Am. Chem. Soc., 2012, **134**, 15197.
15 Z. Zhang, C. Hejesen, M. B. Kjelstrup, V. Birkedal and K. V. Gothelf, J. Am. Chem. Soc., 2014, **136**, 11115.
16 S. A. Jayanthi, A. B. Das and U. Saxena, Biosens. Bioelectron., 2017, **91**, 15.
17 Z. X. Zhou, Q. W. Shang, Y. F. Shen, L. Q. Zhang, Y. Y. Zhang, Y. Q. Lv, Y. Li, S. Q. Liu and Y. J. Zhang, Anal. Chem., 2016, **88**, 6004.
18 J. J. Xu, D. P. Jiang, Y. L. Qin, J. Xia, D. C. Jiang and H. Y. Chen, Anal. Chem., 2017, **89**, 2216.
19 H. Wang, X. S. Sun, D. D. Li, X. D. Zhang, S. C. Chen, W. Shao, Y. P. Tian and Y. Xie, J. Am. Chem. Soc., 2017, **139**, 2468.
20 Q. Zhang, Y. Qiao, F. Hao, L. Zhang, S. Wu, Y. Li, J. Li and X. Song, Chem. Eur. J., 2010, **16**, 8133.
21 M. Faisal, A. A. Ismail, A. A. Ibrahim, H. Bouzid and S. A. Al-Sayari, Chem. Eng. J., 2013, **229**, 225.
22 F. Song, X. L. Hu, J. Am. Chem. Soc., 2014, **136**, 16481.
23 M. Laurenti, M. Paezperez, M. Algarra, P. Alonsocristobal, E. Lopezcabarcos, D. Mendezgonzalez and J. Rubioretama, ACS Appl. Mater. Interfaces, 2014, **8**, 12644.
24 W. Li, J. S. Wang, J. S. Ren and X. G. Qu, J. Am. Chem. Soc., 2014, **136,** 2248.
25 W. Cheng, F. Rechberger and M. Niederberger, ACS Nano, 2016, **10**, 2467.
26 Y. Chen, Y. Wu, B. Sun, S. Liu and H. Liu, Small, 2017, **13**, 1603446.
27 R. Y. Li, R. Yan, J. C. Bao, W. W. Tu and Z. H. Dai, Chem. Commun., 2016, **52**, 11799.
28 Y. W. Liu, X. M. Hua, C. Xiao, T. F. Zhou, P. C. Huang, Z. P. Guo, B. C. Pan and Y. Xie, J. Am. Chem. Soc., 2016, **138**, 5087.
29 J. Swaminathan, R. Subbiah and V. Singaram, ACS Catal., 2016, **6**, 2222.
30 J. F. Xie, J. J. Zhang, S. Li, F. Grote, X. D. Zhang, H. Zhang, R. X. Wang, Y. Lei, B. C. Pa and Y. Xie, J. Am. Chem. Soc., 2013, **135**, 17881.
31 S. L. Liu, Q. H. Zhang, L. Zhang, L. Gu, G. Z. Zou, J. C. Bao and Z. H. Dai, J. Am. Chem. Soc., 2016, **138**, 1154.
32 Z. Chen, Y. Liu, Y. Wang, X. Zhao and J. Li, Anal. Chem., 2013, **85**, 4431.